Electromagnetic Field Measurements on a Millimeter Wave Linear Accelerator

Paul J. Matthews, Timothy Berenc, Frank Schoenfeld, Alan D. Feinerman, *Member, IEEE*, Yoon W. Kang, *Member, IEEE*, and Robert Kustom

Abstract—**Perturbational field strength measurements suitable for use on a proposed 120-GHz 50-MeV electron linear accelerator are described. The measurements are used to determine the R/Q of the device, where R is the shunt impedance. The perturbation is achieved by the use of hollow metallic cylinders with diameters ranging from 25 to 127 μm which are approximately 500 μm long. The cylinders were fabricated by sputtering aluminum through a shadow mask onto silica optical fibers as well as nylon surgical thread. The perturbational "form factors" for such a geometry are experimentally determined using a pillbox cavity. The measured values for the form factors are compared to theoretical estimations, which result in simple analytical expressions. The measured form factors are also compared to values calculated from a finite difference model of the perturbing object. The R/Q for various accelerating modes is measured on a 12-GHz model of the 120-GHz structure. Results are compared to predictions from a finite difference model of the accelerating structure.**

I. Introduction

A LINEAR accelerator is essentially a series of coupled cavities which form a slow wave structure to match the phase velocity of the accelerating mode to the velocity of the particle beam. For efficient operation, an iris loaded cylindrical waveguide geometry is normally employed. The frequency of operation for typical linear accelerators is on the order of a few hundred megahertz, since readily available power sources exist at these frequencies. However, higher frequency linear accelerators have certain distinct advantages such as a relaxation in the power requirements and an increase in the maximum attainable field gradient [1]–[3]. Recent research in the field has focused on the fabrication of compact, high-frequency linear accelerators.

Work is currently underway at the Advanced Photon Source (APS) at Argonne National Laboratory to develop a millimeter wave, 50-MeV electron linear accelerator system [1]. Work is also proceeding on the development of a miniature electromagnetic or microwave undulator. The combination of the two systems would enable the production of a relatively inexpensive, compact, tunable source of coherent synchrotron radiation. Such a system would be extremely useful for various diagnostic and medical purposes.

The proposed millimeter wave electron linear accelerator is designed to operate at 120 GHz. Nominal cavity dimensions are on the order of 1 mm or less with dimensional tolerances of better than 0.1%. Additionally, a device flatness of 1–2 μm per 7 cm and a surface smoothness of better than 0.1 μm are required. Such dimensions and constraints make device fabrication difficult or impossible using conventional techniques. The only fabrication technique currently capable of meeting all of the structural requirements is the so-called LIGA technique developed at the Karlsruhe Nuclear Research Center [4]. LIGA is a German acronym describing the essential fabrication steps in the process—lithography using synchrotron radiation, electroplating, and injection molding (in German: Lithographie, Galvanoformung, Abformung). The use of highly collimated synchrotron radiation enables the LIGA technique to produce extremely accurate patterns in thick resist layers.

In order to make use of the LIGA fabrication technique, the proposed linear accelerator design was modified, which resulted in a double-sided planar "muffin-tin" structure shown schematically in Fig. 1. The device is a constant impedance structure designed for $2\pi/3$ traveling wave operation at 120 GHz. Typical cavity dimensions are given in Table I. Besides allowing for fabrication using the LIGA technique, the planarized design also allows for efficient cooling, provides natural vacuum pumping ports, and allows higher-order mode damping through the side openings.

The effectiveness of an accelerating structure can be described by a few figures of merit. One such figure of merit is the resonant shunt impedance R, which relates the accelerating voltage seen by the particles to the power lost in the structure. The ratio of the shunt impedance to the quality factor, R/Q, is especially useful to compare different accelerator designs since it is loss independent.

For most accelerating structures, the value R/Q is difficult to determine analytically. Typically, numerical methods such as three-dimensional electromagnetic finite difference codes are used to determine the theoretical R/Q of a structure. Experimental determination of R/Q is usually accomplished using a variation of the perturbation technique originally developed by Maier and Slater [5] to measure the accelerating electromagnetic fields. In this technique, the frequency of a closed resonant cavity perturbed by a small object is related to the local electric and magnetic fields at the position of the perturbation. The relation between the resonant frequency

Manuscript received April 10, 1995; revised April 19, 1996.

P. J. Matthews is with the Optical Sciences Division, Naval Research Laboratory, Washington, DC 20375 USA.

T. Berenc, Y. W. Kang, and R. Kustom are with the Argonne National Laboratory, Advanced Photon Source, Argonne, IL 60439 USA.

F. Schoenfeld is with Berliner Elektronenspeichering-Gesellschaft fuer Synchrotonstrahlung mbH (BESSY II), Berlin, Germany.

A. D. Feinerman is with the University of Illinois at Chicago, Chicago, IL 60607 USA.

Publisher Item Identifier S 0018-9480(96)05655-4.

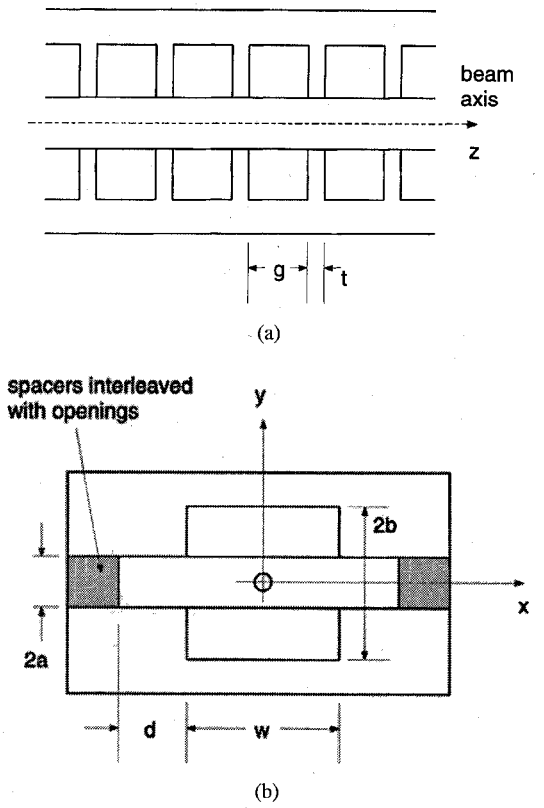

Fig. 1. Schematic view of the proposed millimeter wave linear accelerator.

TABLE I
DIMENSIONS OF THE PROPOSED 120-GHz LINEAR ACCELERATOR SHOWN IN FIG. 1

Parameter	Dimension (μm)
a	300
b	900
w	1800
g	633
t	200
d	800

and the local fields is affected by the size and shape of the perturbing object through the so-called "form-factor." In principle, the perturbing object may be of any shape and may be metallic or dielectric. However, the form factors can be determined analytically only for a few very simple shapes.

For conventional accelerating structures, the perturbing object is usually a small metallic sphere or needle suspended on a thin nylon thread along the particle beam path. The thread should be small enough so that it introduces no noticeable perturbation of its own. The size of the perturbing object or "bead" is chosen such that the perturbation is easily measured but can still be considered a perturbation. Typically, a needle or spheroid with a diameter of $\approx \lambda/500$ and a length of $\approx \lambda/50$ is used. Since the desired operating frequency of our proposed accelerator is 120 GHz, the measurement of the R/Q using conventional perturbing objects is difficult. This paper describes a perturbation technique for performing R/Q measurements on the proposed millimeter wave structure. The perturbing objects are optical fibers and thin nylon threads coated with an aluminum film to form a hollow cylinder with a given diameter and length. The major difficulty with such an approach is evaluating the perturbational form factors for such a geometry.

The general theory of perturbational field strength measurements is presented in Section II. In Section III the fabrication of the novel perturbing bead is described. Section IV discusses measurements and several theoretical predictions for the perturbational form factors of the bead. In Section V, measurements of the R/Q for various accelerating modes of a 12-GHz scale model of the structure are described. Finally, conclusions are given.

II. PERTURBATION THEORY

Perturbational field strength measurement techniques originated with the work by Maier and Slater [5], in which they theoretically derived formulas which related the frequency of a closed resonant cavity to the local fields at the position of a small perturbing object. Formulas were derived for the case of a spheroidal bead made of a conducting material. To derive their formulas, classical solutions were used to obtain the fields as perturbed by spheroidal shells of sufficient thinness such that perturbation theory is valid. Successive applications of this approach to perturbation theory then built up a solid spheroidal bead of sufficient size.

This approach can be generalized to beads of arbitrary ellipsoidal shapes and of arbitrary dielectric material. The fundamental perturbation relation is expressed by [6], [7]

$$\frac{\Delta f}{f_0} = -\frac{1}{4U}\int_{\Delta V} (\boldsymbol{E}_0 \cdot \boldsymbol{P} + \boldsymbol{H}_0 \cdot \boldsymbol{M})\, dV \qquad (1)$$

where f_0 is the unperturbed resonant frequency, $\Delta f = f_0 - f$, U is the energy stored in the cavity, $\boldsymbol{E}_0$ and $\boldsymbol{H}_0$ are the unperturbed electric and magnetic fields of the cavity, and $\boldsymbol{P}$ and $\boldsymbol{M}$ are the induced electric and magnetic polarizations. The integration is taken over the volume of the perturbing object.

If the perturbing object's dimensions are small compared to a wavelength, then equation (1) may be written as

$$\frac{\Delta f}{f_0} \approx -\frac{3\Delta V}{4U}\left[\epsilon_0(F_1|\boldsymbol{E}_\parallel|^2 + F_2|\boldsymbol{E}_\perp|^2) - \frac{\mu_0}{2}(F_3|\boldsymbol{H}_\parallel|^2 + F_4|\boldsymbol{H}_\perp|^2)\right] \qquad (2)$$

where $\boldsymbol{E}_\parallel$ ($\boldsymbol{E}_\perp$) and $\boldsymbol{H}_\parallel$ ($\boldsymbol{H}_\perp$) are the electric and magnetic fields parallel (perpendicular) to the perturbing object axis, and F_i are the perturbational form factors which depend on the material, size, and shape of the perturbing object. Equation (2) is similar in form to the perturbation formula used in [8].

The form factors are easily determined only for a small class of simple shapes. For instance, a metallic sphere exhibits no directional preference and thus the form factors for a metallic sphere are all equal ($F_i = 1$) [5]. The form factors for a general metallic spheroid can also be readily determined and are given by [7]

$$F_1 = \frac{1}{3L_\parallel}$$

$$F_2 = \frac{1}{3L_\perp}$$

$$F_3 = \frac{2}{3 - 3L_{\|}}$$
$$F_4 = \frac{2}{3 - 3L_{\perp}} \tag{3}$$

where $L_{\|}$ and $L_{\perp}$ are the depolarization factors [9] for the directions parallel and perpendicular to the perturbing object axis.

For a prolate spheroid, the depolarization factors are given by

$$L_{\|} = \frac{1-e^2}{e^3}\left[\frac{1}{2}\ln\frac{1+e}{1-e} - e\right]$$
$$L_{\perp} = \frac{1-e^2}{4e^3}\left[\frac{2}{1-e^2} - \ln\frac{1+e}{1-e}\right]$$
$$e = \sqrt{1 - \frac{a^2}{l^2}} \tag{4}$$

where l and a are the axes of the spheroid, l is along the parallel field axis (beam axis), and $l > a$. The depolarization factors for an oblate spheroid are given by

$$L_{\|} = \frac{1+e^2}{e^3}[e - \arctan e]$$
$$L_{\perp} = \frac{1+e^2}{8e^3}\left[\arctan e - \frac{e(1-e^2)}{(1+e^2)^2}\right]$$
$$e = \sqrt{\frac{a^2}{l^2} - 1} \tag{5}$$

where $l < a$.

In accelerating structures, one is concerned with measuring the R/Q of the accelerating mode along the beam path. The transit time corrected shunt impedance R is defined as [10]

$$R = \frac{\left|\int E_z(x, y, z)e^{i(\omega z/v)}\,dz\right|^2}{P} \tag{6}$$

where E_z is the field along the beam path, P is the power dissipated in the walls of the structure, and v is the velocity of the particles. The quantity in the numerator is simply the square of the voltage gain of the particle after traversing the accelerator. The R/Q of the structure can then be expressed as

$$\frac{R}{Q} = \frac{1}{\omega U}\left[\left(\int E_z \cos kz\,dz\right)^2 + \left(\int E_z \sin kz\,dz\right)^2\right] \tag{7}$$

where use was made of Euler's law and $k = \omega z/v$.

In accelerating structures, one is normally concerned only with modes which have only an electric field component parallel to the beam (E_z) along the beam path and no magnetic fields. Solving (2) for E_z ($E_{\|}$), with all other fields equal to zero, and substituting into (7) gives

$$\frac{R}{Q} = \frac{2}{3\pi f_0 \Delta V F_1 \epsilon_0}\left[\left(\int\sqrt{\frac{\Delta f}{f_0}}\cos kz\,dz\right)^2 + \left(\int\sqrt{\frac{\Delta f}{f_0}}\sin kz\,dz\right)^2\right] \tag{8}$$

where f_0 is the resonant frequency of the mode. The measurement of the R/Q of the structure is reduced to a simple measurement of the frequency shift of the accelerating mode resonance due to the presence of the perturbing object at each point along the particle beam path. It should be noted that (2) allows one to determine the square of the magnitude of the fields only. Thus, there is an uncertainty in the determination of the sign of the square root in (8) which is usually handled through previous knowledge of the expected field distribution.

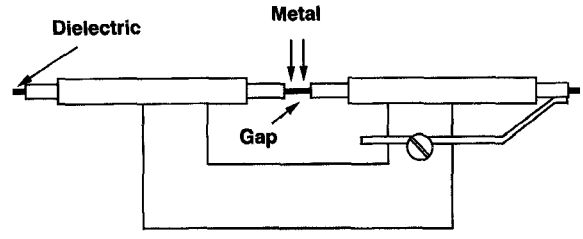

Fig. 2. The fabrication fixture.

III. Fabrication

The microfabrication of a submillimeter hollow cylinder presents an interesting challenge since most of the processes and tools for fabrication on this scale are normally used with planar substrates. After some experimentation, a suitable technique was discovered. The technique involves depositing a metal film on a dielectric rod which has been masked to define the cylinder length. This was accomplished with the use of a specially designed fixture shown in Fig. 2. The dielectric rod is threaded through two coaxial copper tubes. The ends of the tubes on either side of the gap have 150-μm orifices to prevent metal from depositing anywhere on the rod except within the gap. The size of the gap can be adjusted to vary the bead length. The bead inner diameter is determined by the dielectric outer diameter.

Initially, beads were fabricated on silica single mode optical fibers. Optical fiber was chosen for its small, uniform (typically 0.1%/km) diameter [11]. The silica fibers were found to be quite fragile once the polymer buffer layer was removed to expose the 80-μm fiber. Nylon thread was then used since it is more flexible and commercially available with diameters ranging from 25 to 127 μm.

In order to achieve complete coverage of the metal film around the dielectric rod, the entire fixture was rotated 90° about an axis parallel to the thread between each of four depositions. The distance between the target and the thread varied from 10 to 15 cm, depending upon the position of the fixture since the rotation and thread axis were offset. The sputtering rate was measured and the deposition at each position would have resulted in a 0.6-μm-thick film on a flat substrate 10 cm from the target. The bead thickness was estimated to range from 0.3 to 0.7 μm, assuming that the target is an extended source of aluminum atoms. This nonuniformity around the bead circumference is due to the target to thread distance variation and the variation in the angle between the incident atoms and the normal to the bead surface. The aluminum was sputtered in an argon atmosphere at a pressure of 1.5×10^{-3} Torr, giving a mean free path of the aluminum

atoms of ≈ 5 cm. The scattering at this pressure should not significantly change these estimates.

IV. Form Factor Calibration Techniques

Accurate R/Q measurements require a precise knowledge of the form factors of the perturbing object. Unless the object is a spheroid, simple analytical expressions for the form factors do not exist. This is the major difficulty associated with using the cylindrical bead described in the previous section. The form factors may be determined using a variety of methods which are described in this section. The results will be compared at the end of the section.

A crude approximation for the form factors may be obtained by considering the hollow, metallic cylinder which has a given length $2l$, and diameter $2a$, to be a spheroid of major axis l, and minor axis a. By making this approximation, one can use the formula of (4)–(6) to estimate the form factors for a hollow, metallic cylinder. Due to the differences in geometry between cylinders and spheroids, this approach is very inaccurate for aspect ratios, l/a, near one and would converge to the correct solution for very large aspect ratios.

The problem of the perturbation due to an infinitely thin hollow cylinder was solved in [12] and [13]. The problem is described by a Fredholm integral equation of the first kind, which is then transformed into an infinite system of linear equations using the method of moments. The infinite linear system is solved by truncating to a reasonable number of equations and unknowns (one), and extrapolating the results to an infinite system by assuming a polynomial dependence on the number of equations. The following simple analytical expression was arrived at for the first form factor of a hollow, metallic cylinder:

$$F_1 = \frac{2}{9}\left(\frac{l}{a}\right)^2 \ln\left[\left(\frac{2}{3\pi}\frac{l}{a}\right) + \sqrt{\left(\frac{2}{3\pi}\frac{l}{a}\right)^2 + 1}\right]^{-1} \tag{9}$$

where $2l$ and $2a$ are the length and diameter of the cylinder. Similar to the spheroidal approximation, equation (9) is accurate for $l/a \to 0$ or $l/a \to \infty$. The error is claimed to be less than $\pm 9\%$ for $0.68 < l/a < 18.3$.

The form factors may also be found using numerical methods. If our perturbing cylinder is situated in an electric field parallel to the cylinder axis with no magnetic field, then (2) may be solved for the first form factor.

$$F_1 = -\frac{\Delta f}{f_0}\frac{4U}{3\Delta V \epsilon_0 |E_\parallel|^2}. \tag{10}$$

If the frequency shift due to the perturbation can be computed, then the first form factor may be calculated. This is accomplished by calculating the resonant frequencies of a closed cavity with and without a perturbing hollow, metallic cylinder using a finite difference technique.

A standard pillbox cavity was modeled since the modal fields are readily calculable. The TM_{010} mode closely resembles the desired accelerating modes of the proposed structure and has only a longitudinal electric field on axis. The electric field of the TM_{010} mode is given by

$$E_z = E_0 J_0\left(p_{01}\frac{r}{a}\right) \tag{11}$$

where E_0 is the peak field, J_0 is a zero-order Bessel function of the first kind, p_{01} is the first root of the Bessel function, a is the radius of the cavity, and r is the distance from the cavity axis. The total energy stored in the TM_{010} mode is given by

$$U = \frac{\epsilon_0}{2}\int_V |E(x, y, z)|^2\, dV = \frac{\epsilon_0}{2} E_0^2 V J_1^2(p_{01}). \tag{12}$$

Equation (12) may be substituted into (10) to give

$$F_1 = -\frac{\Delta f}{f_0}\frac{2V J_1^2(p_{01})}{3\Delta V} \tag{13}$$

where the cavity and perturbing bead axis are aligned such that $E_z = E_\parallel$.

A pillbox cavity with a 9-mm radius and a 6-mm length was modeled using the URMEL [14] finite difference code. URMEL is capable of modeling cylindrically symmetric structures in the time and frequency domains. A suitable mesh was chosen, and the unperturbed resonant frequency of the TM_{010} mode of the cavity was calculated. The resonant frequency was then calculated for the case of a perturbing metallic cylinder on the cavity axis. The results were substituted into (13) to arrive at the form factor. Various aspect ratios for the perturbing cylinder were chosen. Both hollow and solid perturbing cylinders were investigated. Results are given in Table II.

TABLE II
The Form Factor F_1 Calculated Using URMEL. A 40-μm Diameter Hollow Cylinder Was Used as the Perturbation

Aspect Ratio	F_1
1.25	1.72
2.50	3.26
3.75	5.03
5.00	6.95
6.25	9.19
7.50	11.61
8.75	14.31
10.00	17.15
11.25	20.20
12.50	23.47
15.00	30.59
17.50	38.46
20.00	47.10

It was discovered that the hollow cylinder resulted in a form factor slightly smaller than a solid cylinder due to penetration of the field into the TM waveguide modes of the cylinder. This results in an effective shortening of the length of the cylinder. The length was decreased by the distance over which the fields of the TM_{01} mode of the waveguide were down by approximately 20%. The result is negligible ($< 2\%$) for beads with a diameter of 100 μm and an aspect ratio greater than 3. The difference will obviously decrease for smaller diameter cylinders which have TM_{01} modes further from cutoff. However, for any given cylinder geometry, the results of the numerical simulation are expected to be very good. The results will be discussed at the end of the section.

TABLE III
THE FORM FACTOR F_1 MEASURED USING COPPER TUBING AND A 348-MHz ALUMINUM PILLBOX CAVITY

Aspect Ratio	F_1
2.98	3.43 ± 0.02
3.23	3.75 ± 0.04
4.00	4.76 ± 0.02
4.96	6.40 ± 0.05
5.85	8.00 ± 0.05
7.00	10.12 ± 0.06
8.00	12.04 ± 0.06
8.96	13.76 ± 0.10
10.05	16.39 ± 0.06
11.06	18.86 ± 0.14
12.09	21.49 ± 0.11
12.76	22.87 ± 0.45

The form factors may also be calibrated by measuring them in a cavity with a known or calculable field distribution. This approach is similar to the numerical simulation discussed above except that the frequency difference is directly measured in a test cavity. Again, a pillbox cavity is used along with (13). The pillbox used was a 348-MHz aluminum cavity 66.0 cm in diameter and 37.5 cm long with an unloaded Q of approximately 24 000. This cavity was used since it was more stable thermally and vibrationally than higher frequency cavities. The perturbing beads were simulated by using 1.19- to 2.74-mm-diameter copper tube cut to various lengths and suspended on a 1-mm-diameter nylon thread. These beads were easy to fabricate and simulated rather well the beads used at higher frequencies.

The change in resonant frequency can be measured either directly by measuring the perturbed resonant frequency at each position of the perturbing object along the cavity axis, or indirectly by measuring the phase of a transmitted signal at f_0. A discussion of the merits of the two methods can be found in [6], [13], [12] and various other sources. If the phase is set equal to zero at the unperturbed resonant frequency and the frequency shift is small (<45°), then the perturbed frequency is given by

$$\frac{\Delta f}{f_0} = \frac{\tan\phi}{2Q_L} \tag{14}$$

where ϕ is the phase of the transmitted signal and Q_L is the loaded Q of the cavity. The indirect phase technique using a network analyzer was used for all measurements since it is inherently faster and thus reduces temperature induced frequency drift. Results for various aspect ratios are listed in Table III. The listed error is the standard deviation of four measurements.

Some sources of error in the measurement include accuracy in determining the unperturbed resonant frequency, accuracy in the phase measurement, perturbations due to the nylon thread, thermal drift of the cavity resonance, field distortion due to the perturbation measurement port openings, and accuracy in determining the loaded Q of the cavity. Experimentation showed that the unperturbed resonant frequency could be determined to about ±300 Hz over the time of the measurement which has a negligible effect on measurement accuracy. The phase change could be measured to an accuracy of approximately 1%. Errors due to misalignment to the center of the cavity are minimized by the use of such a large cavity.

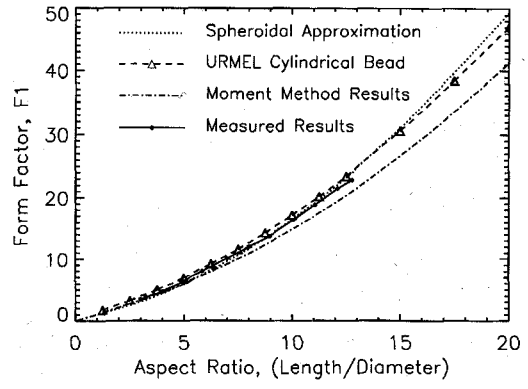

Fig. 3. A comparison of the various techniques to determine F_1.

The cavity resonant frequency was not noticeably changed by the introduction of a bare nylon thread. Thermal drift was minimized by shielding the measurement area with a thick vinyl hood and keeping measurement time to about 10 minutes. Steady temperature drifts could be compensated by postprocessing the data. Field distortions due to the measurement port openings were minimized by calculating the phase change only over the central region of the cavity. Using averaging techniques, the loaded Q of the cavity could be determined to about ±2%. Given all of the errors involved, the accuracy of the measurement technique is estimated to be approximately 5%.

The four techniques for calculation of the form factor of a hollow, metallic cylinder are compared graphically in Fig. 3. The experimental results are fit to a second-order polynomial given by

$$F_1 = 0.0615\left(\frac{l}{a}\right)^2 + 1.041\frac{l}{a} - 0.267 \tag{15}$$

where a least squares method was used. The percent deviation of (15) from the measured data is shown in Fig. 4. The deviation of the various approximations from (15) is plotted in Fig. 5. Aspect ratios below approximately 3 are probably not valid since the extrapolation of (15) to these values is questionable. Examination of the results shows that the spheroidal approximation is too low over the range $3 < l/a < 10$, and too high for aspect ratios greater than 10. The deviation lies within about ±10% of the measured values. The URMEL results, which are expected to be very accurate, are approximately 5% higher than the measured results but seem to improve with increasing aspect ratio. The approximation of equation (9) gives results that are generally lower than the measured form factor by about 10% for all aspect ratios. Given this comparison, it appears that the form factors should be measured for the precise determination of the R/Q of a structure.

V. MEASUREMENTS

Measurements of device R/Q were performed on a 12-GHz copper scale model of the proposed device. Since R/Q

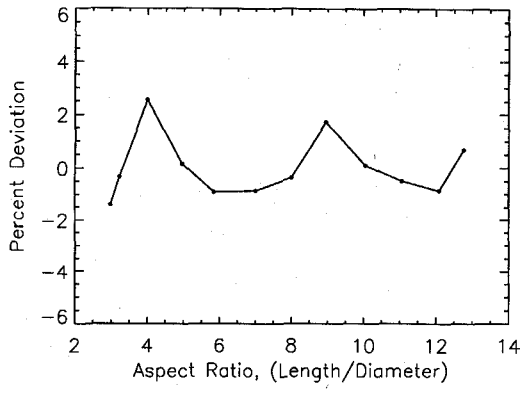

Fig. 4. The percent deviation of the polynomial fit to the measured data.

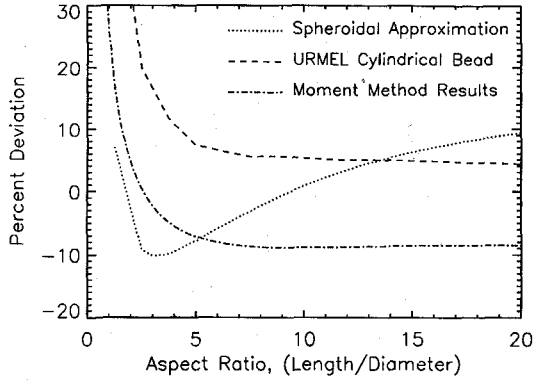

Fig. 5. The percent deviation of the various theoretical methods of determining F_1 from the measured data.

is loss independent and scales directly with frequency, the results at 12 GHz are applicable to the actual 120-GHz wave device. A frequency of 12 GHz was chosen so that many of the difficulties which will arise at 120 GHz will be encountered. Each half of the 12-GHz model was fabricated by machining the cavities through a 6-mm copper plate and then soft soldering the plate to a copper substrate. The gap between the halves was maintained using spacers. The traveling wave structure was then transformed into a resonant cavity by introducing shorting planes within the device. For accelerating modes, the shorting planes should reside at the center of each cavity. Since we are interested in the $2\pi/3$ mode (120° phase shift per cell) which has a characteristic guide wavelength equal to three cells, the total number of cells enclosed by the shorting planes should be a multiple of three.

The shorting planes were designed with a 0.508-mm aperture on the beam axis to allow the perturbing cylinder and fiber to be pulled through the cavity. The resulting resonant structure was excited through two coaxial electric field probes located in the shorting planes 6.35 mm from the beam axis. The probes had an outer diameter of 1.194 mm. The inner and outer conductor radii are 0.152 and 0.508 mm, respectively. The probe size and position were carefully chosen to minimize distortions to the mode. Additionally, the shorting planes must be positioned precisely at the center of the cell in order to properly excite the correct mode and avoid field distortions.

Cylindrical aluminum beads were fabricated using the techniques described in Section III. Nylon lines ranging from 25 to 127 μm in diameter and 80-μm-diameter optical fiber were used. Bead lengths ranged from approximately 400 to 600 μm.

TABLE IV
MEASURED FORM FACTORS FOR THE BEADS USED ON THE 12-GHz MODEL

Diameter (μm)	Length (μm)	Measured F_1	Predicted F_1 (Equation 15)
25	514	46.07	45.98
51	521	16.42	16.88
80	510	9.16	8.87
102	531	7.62	6.82
127	577	5.07	5.73

To ensure accuracy in the final results, the form factors were measured as in Section IV using a 12-GHz copper pillbox cavity. Care was taken to thermally stabilize the cavity during the measurements. The fibers were held by optical fiber chucks and positioned using 0.1-μm-resolution manual micropositioners. A stepping motor with a 0.1 μm minimum step size was used to pull the bead through the cavity. The measurement technique is identical to the one described in the previous section. Again, the indirect phase measurement method of (14) was used to calculate the frequency change.

Due to the fabrication methods used on the 12-GHz pillbox cavity, the field for the TM_{010} was not uniform across the cavity but gradually decreased from one end to the other. This resulted in a 10% phase variation. The measured form factors were calculated by using the average phase across the cavity. The results are shown in Table IV. Table IV also compares the results to equation (15) which was obtained from beads measured on the more stable 343 MHz cavity. The 25- and 51-μm-diameter beads were fabricated on surgical thread and closely match the results of equation (15). The 102- and 127-μm-diameter beads were fabricated on nylon lines and show much more variation than equation (15). This may be due to variations in the uniformity of the dielectric constant of the nylon lines or to the larger diameter of the line.

Measurements were taken on the 12-GHz linear accelerator model using the measured form factors from Table IV. The beads were positioned and measurements taken as described above. As previously mentioned, the number of cells measured should be a multiple of three. The number of cells chosen has some effect on the results. If too few cells are chosen, the field distortions due to the shorting planes can be large. However, if too many cells are used, the number of allowed modes increases and the mode spacing is decreased. Also, a large number of cells leads to a larger stored energy which decreases the measured signal allowing noise to affect the results.

The results of the measurements are shown in Table V. A typical measurement on nine cells is shown in Fig. 6. As expected, measurements on only three cells gives a slightly lower value for R/Q due to the perturbations of the shorting planes. One can see this effect by noticing the decrease in phase change for the end cells in Fig. 6. As the number of cells is increased, the effect of the shorting planes is reduced and the measured R/Q approaches the true measured value. This value is approximately 8.1 kΩ/m, which is 45% lower than the theoretical result.

TABLE V
RESULTS OF THE R/Q MEASUREMENTS

Number of Cells	R/Q (kΩ/m)	Percent Difference
3	7.785	-46%
6	7.938	-45%
9	7.820	-46%
12	8.363	-42%
15	7.861	-46%
18	8.271	-43%
Theoretical	14.45	–

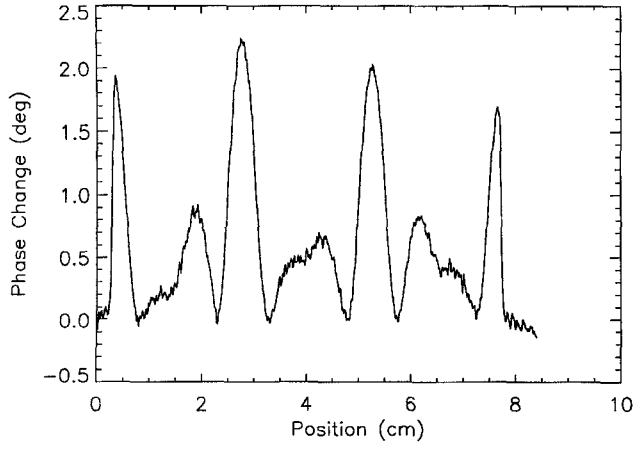

Fig. 6. Perturbation measurement results of the $2\pi/3$ mode for nine cells of the 12-GHz model.

TABLE VI
ACTUAL DIMENSIONS OF THE 12-GHz SCALE MODEL

Dimension	Design	Average	Standard Deviation	Low	High
w (mm)	18.00	18.03	0.029	17.98	18.08
g (mm)	6.33	6.40	0.0196	6.38	6.48
t (mm)	2.00	1.90	0.0069	1.91	1.89
a (mm)	6.00	6.00	0.0078	5.99	6.01

The large reduction from the theoretically predicted result can be traced to several factors. One factor is the uniformity and precision of the machined cavities. In general, geometrical tolerances for a normal linear accelerator must be maintained to approximately 1 part in 1000. Even with these tolerances, a typical linear accelerator must be mechanically tuned, section by section. Table VI shows the measured dimensions of the test structure. Tolerances are acceptable for the most part, but worse than 1:1000. Additionally, the two halves of the structure were difficult to align properly and may have been skewed with respect to one another. Even a slight skew between the two halves of the structure would result in a large reduction in the measured R/Q. The machined scale model made no provisions for the precise alignment of the halves. Also, no mechanical tuning is possible with this structure. In order to do away with the need for mechanical tuning, the device mechanical tolerances should approach 1:5000 to 1:10 000. These problems can significantly degrade the R/Q of a structure. The actual 120-GHz device will most likely have significantly better tolerances and will not need tuning as a result of the fabrication methods being employed [1].

A second factor, which is again related to the mechanical tolerances and fabrication of the test structure, is the presence of various structural deformities in the cavities. As mentioned earlier, each half of the device was fabricated by soft soldering two pieces. The soldering procedure left behind small nonuniformities and "bumps" at the interface between the two pieces. These perturbations can severely affect the R/Q, and are not reflected in the mechanical tolerance measurements.

Another source of error, mentioned previously, was the presence of the shorting planes which contained apertures to pass the bead and hold the input excitation probes. Apertures of various sizes were used, and the size of these apertures was observed to have a direct effect on the measured R/Q. The probes used were the smallest commercially available coaxial lines. The bead aperture was made as small as was feasible for the threads used. The data of Table V do not indicate that measuring longer structures appreciably decreases the measured effect of the shorting planes. This is most likely due to the increased effect of the mechanical nonuniformities and defects in the structure which are more apparent for a larger number of cavities.

At 120 GHz, the shorting plane and excitation problems will be much more severe. Shorting planes machined as separate pieces and inserted into the device will not be practical. An alternative approach would be to design a resonant micromachined structure for testing purposes which is identical to the desired traveling structure. The two structures can be fabricated during a single micromachining run so that they have similar mechanical tolerances. The aperture for the bead as well as the bead can be scaled appropriately. Special optical fibers with diameters of 5–10 μm can be used. Also, coaxial probes cannot be used at 120 GHz, and alternative excitation techniques such as evanescent wave side coupling must be employed.

The nonuniformities in the bead film thickness described earlier can also affect the results especially if the bead has a different rotational position between the form factor calibration measurement and the actual device measurement. Finally, environmental factors such as temperature can affect the results. Most measurements displayed a steady temperature drift which could be compensated. However, properly insulating the setup from temperature and vibrational effects should improve the results.

VI. CONCLUSION

A perturbational technique was investigated for use in measuring the electric field distribution in high-frequency linear accelerators currently under development. The perturbing object was a hollow aluminum cylinder fabricated on small-diameter nylon threads and glass optical fibers. A novel masking and sputtering technique was utilized for fabrication of the perturbing bead. The perturbational form factors for the fabricated beads were calculated theoretically using several techniques. The computed form factors were then compared to measured values. The form factors were measured in a 348-MHz aluminum pillbox cavity using copper tubing of various diameters and lengths to simulate the miniature beads.

The perturbational technique was then used to calculate the R/Q of a 12-GHz model of a proposed millimeter wave linear accelerator. The device was designed for $2\pi/3$ mode traveling wave operation. Cylinders with diameters from 25 to 127 μm and lengths of $\approx$500 μm were used as the perturbing objects. The measured R/Q for the $2\pi/3$ mode was 8.1 kΩ/m, which is about 45% less than theoretically predicted. The difference was mainly attributed to imperfections in the fabrication and alignment of the scale model. The technique appears feasible for use at the actual device operating frequency of 120 GHz.

REFERENCES

[1] A. Nassiri, R. L. Kustom, F. E. Mills, Y. W. Kang, A. D. Feinerman, H. Henke, P. J. Matthew, T. L. Willke, D. Grudzien, J. Song, and D. Horan, in *Proc. IEEE Int. Electron Device Meet.*, Washington, DC, Dec. 1993, pp. 111–120.

[2] P. B. Wilson, "Application of high-power microwave sources to TeV linear colliders," in *Application of High-Power Microwaves*, A. V. Gaponov-Grekhov and V. L. Granatstein, Eds. Norwood, MA: Artech House, 1994.

[3] *The Stanford Two-Mile Accelerator*, R. Neal, Ed. New York: W. A. Benjamin, 1968.

[4] E. W. Becker, W. Ehrfeld, P. Hagmann, A. Maner, and D. Münchmeyer, "Fabrication of microstructures with high aspect ratios and great structural heights by synchrotron radiation lithography, galvanoforming and plastic moulding (LIGA process)," *Microelectron Eng.*, vol. 4, pp. 35–36, 1986.

[5] L. C. Maier and J. C. Slater, "Field strength measurements in resonant cavities," *J. Appl. Phys.*, vol. 23, pp. 68–77, 1952.

[6] H. Hahn and H. J. Halama, "Perturbation measurement of transverse R/Q in iris-loaded waveguides," *IEEE Trans. Microwave Theory Tech.*, vol. MTT-16, pp. 20–29, 1968.

[7] T. Khoe, "The effect of small ellipsoidal material on the resonant frequency of a cavity," Advanced Photon Source Rep. LS-179, 1991.

[8] J. Jacob, "Measurement of the higher order mode impedances of the LEP cavities," European Synchrotron Radiation Facility (ESRF) Rep. ESRF-RF/88-02, 1988.

[9] M. Mason and W. Weaver, *The Electromagnetic Field.* New York: Dover, 1929.

[10] *Linear Accelerators*, P. M. Lapostolle and A. L. Septier, Eds. Amsterdam: North-Holland, 1970.

[11] J. Gowar, *Optical Communication Systems.* London: Prentice-Hall, 1984.

[12] F. Caspers and G. Dôme, "Precise perturbation measurements of resonant cavities and higher order mode identification," CERN Rep. SPS/85-46, 1985.

[13] ——, presented at the *1984 Conf. Precision Electromagnetic Meas.*, Delft, The Netherlands, 1984.

[14] T. Weiland, "On the computation of resonant modes in cylindrically symmetric cavities," *Nuclear Instr. Methods*, vol. 216, pp. 329–348, 1983.

Paul J. Matthews received the B.S. degree (magna cum laude) in physics from Loyola University of Chicago in 1986, and the M.S. and Ph.D. degrees in electrical engineering from the University of Colorado in 1988 and 1991, respectively. His Ph.D. dissertation centered on the fabrication and characterization of $LiNbO_3$ and $LiTaO_3$ integrated optical devices for microwave applications.

From January 1992 to October 1992 he was employed by CAI/Recon Optical. In October 1992 he joined the staff of the Advanced Photon Source at Argonne National Laboratory where he was engaged in efforts to design, model, and fabricate a millimeter wave linear accelerator using deep-etch X-ray lithography techniques and electroplating. Since September 1995 he has been with the Optical Sciences Division of the Naval Research Laboratory where he is currently investigating optical control schemes for phased array radar applications.

Timothy Berenc, photograph and biography not available at the time of publication.

Frank Schoenfeld received the degree in electrical engineering from the Technische Universitaet Berlin in 1993.

He is currently a Ph.D. student employed at Berliner Elektronenspeichering-Gesellschaft fuer Synchrotonstrahlung mbH (BESSY II) in Berlin where he is studying higher-order mode damping in accelerator cavities.

Alan D. Feinerman (M'94) received the B.S. degree in engineering and applied physics from Cornell University in 1978, and the M.S. and Ph.D. degrees in physics from Northwestern University in 1983 and 1987. His Ph.D. thesis was on the fabrication and electrical characterization of submicron tungsten interconnects used in integrated circuits.

He is presently an Associate Professor at the University of Illinois at Chicago in the Electrical Engineering and Computer Science Department where he is a participant in the UIC Microfabrication Applications Laboratory. He is developing several manufacturing technologies capable of producing three-dimensional semiconductor/insulator/polymer/metal structures with an accuracy approaching 1 μm by combining semiconductor processing and fiber optic technology. This technology is currently being applied to the miniaturization of the scanning electron microscope, linear accelerator, and other analytical instruments.

Dr. Feinerman is a member of the American Physical Society, American Vacuum Society, Electrochemical Society, and SPIE.

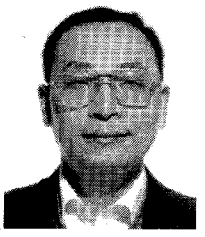

Yoon W. Kang (M'94) received the B.E.E.E. and M.E.E.E. degrees from Yonsei University in Seoul, Korea in 1972 and 1974, respectively; the M.S.E.E. degree from the University of California–Santa Barbara in 1983; and the Ph.D.E.E. from the University of Massachusetts–Amherst in 1986. During his Ph.D. study, he performed research on the numerical analysis, radiation pattern synthesis, and optimization of transient radiation from array antennas.

From 1974 to 1980 he worked with the Agency for Defense Development of Korea as a Microwave Systems Engineer. In 1986 he joined the GE Medical Systems Group where he engaged in the development of near-field antennas and RF subsystems for magnetic resonance imaging systems. From 1989 to 1991 he worked with the GE Astrospace Division, for microwave subsystem development and spherical near-field measurement of antenna systems for communication satellites such as the NASA Advanced Communication Technology Satellite (ACTS). In 1991 he joined the Advanced Photon Source (APS) project, the 7-GeV synchrotron radiation light source at Argonne National Laboratory where he is engaged in the research and development of RF/microwave/millimeter-wave systems for charged particle accelerators and accelerator related systems. His research interests include normal and superconducting electromagnetic cavity structures, microfabrication of millimeter wave amplifiers and devices using deep-etch X-ray lithography, and electromagnetic fields for undulators and free electron lasers.

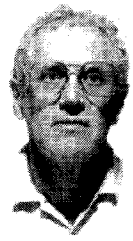

Robert Kustom received the B.S.E.E. and M.S.E.E. degrees from Illinois Institute of Technology in 1956 and 1958, respectively, and the Ph.D.EE from the University of Wisconsin–Madison in 1969.

He worked for three years at the High Voltage Research Laboratory of the Joslyn Manufacturing Company, and for the last 37 years with Argonne National Laboratory. He has worked on the development of elementary particle detectors and radio frequency particle separators, high energy proton accelerator systems, superconducting magnetic systems, and Tokamak fusion energy devices. At Argonne National Laboratory, he was Associate Division Director of the Accelerator Systems Division for five years, and Division Director for two years. He was acting Division Director of the Advanced Photon Source, Accelerator Systems Division, for two years. He currently is Group Leader of the RF Group of the Advanced Photon Source, Accelerator Systems Division, and concurrently holds the position of Adjunct Professor in the ECE Department of the University of Wisconsin–Madison.